Conference Paper, Published Version

Minor, B.; Rennie, Colin D.; Townsend, D. R.

Barbs (Submerged Groynes) for River Bend Bank Protection: Application of a Three-Dimensional Numerical Model

Barbs (Submerged Groynes) for River Bend Bank Protection: Application of a Three-Dimensional Numerical Model

B. Minor*, C.D. Rennie* and D.R. Townsend*
* University of Ottawa/Department of Civil Engineering, Ottawa, Canada

INTRODUCTION

Barbs are low-profile linear structures that are primarily used to prevent the erosion of stream banks. They are a variation of a groyne, similar to spur dikes and bendway weirs. Historically, groyne structures have been built such that the groyne emerges out of the water and is overtopped only at the highest flows. More recently, there has been interest in low-profile submerged groynes, such as barbs, because they require less material to construct and are less obtrusive. Barbs are typically anchored, in series, to the outside bank in stream bends and extend in an upstream direction from the bank into the flow. A unique feature of barbs is that they have trapezoidal cross-sections and that the top of the barb gently slopes downward as it extends away from the bank [1]. A series of barbs is designed to redirect flow away from the outer stream bank and disrupt the velocity gradient and shear stress distribution close to the outer bank. As a result of this disruption the location of the thalweg shifts away from the outside bank. Furthermore, a zone of subcritical flow is generated upstream of the barb structure along the outer bank. Thus a series of barbs, installed correctly, protects the outer bank from erosion and promotes sediment deposition. In addition to this, it has been observed that vortices are generated at the tips of the barbs creating local scour holes that can enhance aquatic habitat [2].

Many field installations of these structures have been performed using good judgment and experience rather than following specific criteria. In addition, there is limited documentation of the design criteria that have been used for the field installation of barbs and for the long-term performance of these structures. Recently there has been an effort to provide recommendations and guidelines for the design of barbs (e.g. [1]). However, it must be noted that these are only suggestions. There remains a need for studies to identify the optimum barb dimensions, spacing, and orientations in the bend flow field for different bend geometries and hydraulic conditions. Furthermore, an understanding of the interaction between the complex flow field and the sediment transport through the channel bend is required in order to predict the long-term performance of these structures.

There have been both laboratory and numerical studies performed on groyne structures. However, most of these studies have been limited to the examination of a single, emergent groyne perpendicular to the stream bank in a straight channel (e.g. [3], [4], [5], and [6]). The studies which have been conducted on groyne fields typically investigate only groynes perpendicular to the flow field. Reference [7] examined flow patterns in a series of emergent perpendicular groynes in a straight channel. Reference [8] described changes in bed morphology due to the installation of a series of groynes in the field. Scour around a single submerged spur dike in a straight channel has recently been studied for orientations perpendicular to the bank [9] and angled upstream [10]. Recently, [11] analyzed flow around a single submerged weir in a channel bend. In 2004 a laboratory study was conducted that examined the scour patterns, in a hydraulically narrow channel, of barb fields in 90^o and 135^o bends with varied spacing and angles of barbs [12].

A three-dimensional numerical model was used to simulate the turbulent flow field and associated scour and deposition of the bed sediments due to a series of barbs in both a 90^o channel bend and a 135^ochannel bend. The numerical model was calibrated to the scour measurement data obtained from the physical laboratory experiments described in [12]. The parameters that were varied for each experiment were channel bend angle, barb alignment, and the location of the barbs in channel bend. This paper aims to: (i) validate the application of a three-dimensional numerical model to moveable-bed bend sections of a hydraulically narrow rectangular channel containing barbs; (ii) simulate the effects of different arrangements of barb groups in the bend section; and (iii) analyze the data to determine the relation of the flow field to associated scour and deposition in a complex fluvial environment. This novel data is useful for improved analyses of the bank protection capabilities of these structures and for the development and improvement of design guidelines.

NUMERICAL MODEL

The three-dimensional numerical model used for this study was Sediment Simulation in Intakes with Multiblock option (SSIIM), Version 1.1. This model, developed at the Norwegian University of Science and Technology [13], uses a three-dimensional structured and non-orthogonal grid. The model utilizes a rigid-lid by default. The three-dimensional Reynolds-averaged Navier-Stokes equations are solved to calculate the water flow. The SIMPLE method [14] is used to solve the pressure term. The Reynolds stresses are solved using the k-ε model, and the suspended sediment transport is calculated with the convection-diffusion equation. The volumetric bedload transport is calculated using van Rijn's bedload transport formula [15].

EXPERIMENTAL DATA

The scour measurement data that is presented in [12] was collected in the Engineering Hydraulics Laboratory at the University of Ottawa. The channel that was used for the testing was comprised of three rectangular-shaped sections; the entrance section was 0.460 meters wide by 0.254 meters deep by 9.75 meters long; the exit section was 0.460 meters by 0.406 meters by 2.44 meters long; and there were two exchangeable bend sections 0.460 meters wide by 0.406 meters deep which were installed separately. The two bend angles used were 90^o and 135^o. The exit sections and the bend section were 0.152 meters deeper than the rest of the channel. This allowed for a 0.152 meter deep sand bed to be placed in the bend and exit sections.

The experimental procedures were largely based on design recommendations by [16]. The parameters that were varied for each experiment were channel bend angle, barb alignment, and the location of the barbs. Judging the effectiveness of the different barb groups in promoting long term stability of the outside bank region was based on two criteria: (i) percent reduction achieved in scouring in the vicinity of the outside bank and (ii) degree to which the channel thalweg was moved from the outside bank region towards the center of the channel. Scour tests were performed separately with the 90^o channel bend section and the 135^o channel bend section. For each channel bend section there were three different barb alignment angles ($\theta = 20^o, 30^o, 40^o$) assessed, where θ is defined as the angle between the tangent line to the bank and the barb. For the 90^o channel bend three different group-types (A, B, and C) were evaluated. Two different group-types were examined in the 135^o channel bend. The group-types (A, B, and C) were defined by the location of the first barb in the group.

The height of the barbs at the bank was half of the mean flow depth and decreased with a 10^o slope away from the bank. The sand placed in the 0.152 meter deep bend and exit sections had a median diameter of 0.85 millimeters with a geometric standard deviation of approximately 1.3. Throughout the experiments, a constant discharge of 0.0132 cubic meters per second was maintained with an average flow depth of 0.102 meters. Further details of the experimental methods and data are available in [12] and [17].

NUMERICAL SIMULATION

90^o Channel

The three-dimensional numerical model was initially used to simulate the sediment transport and flow through the 90^o channel bend without barbs in place. This was performed to calibrate the model before adding the barbs to the channel. A structured grid containing 123 cells in the longitudinal direction, 18 cells in the transverse direction, and 12 cells in the vertical direction was used. In order to remain consistent with the experimental data, the channel geometry, discharge, flow depth, channel slope, and sediment grain size were the same as those measured in the laboratory. For the 90^o channel without barbs the laboratory experiments were run for approximately 26 hours. A simulation time of 15 hours was used for the numerical modeling. The parameters varied to calibrate the numerical model to the experimental data were the bed roughness and the time step. A Manning number of 0.0167 and a time step of 50 seconds proved to yield favorable results. Please note that in all figures the direction of flow is from left to right.

Figure 1 presents a contour map of the predicted bed elevations in meters. These results compare favorably to the bed elevations measured in the laboratory. The laboratory bed elevations are shown in Figure 2. The distribution of boundary shear stress across a channel bend section is complex due to the transverse shear produced by the secondary currents. The secondary flow cell is typically directed vertically down towards the toe of the outside bank. There is an increase in the shear stresses in the outer bank region which results in erosion in the outer bank region. Conversely, there is a decrease in velocity and shear stress along the inside bank which encourages deposition of sediment and the formation of point bars. The laboratory results presented in Figure 2 clearly show these features. From Figure 1 it can be seen that these patterns of sediment deposition and erosion through the bend are sufficiently simulated by the numerical model. The location and magnitude of the measured and predicted point bar are observed to be comparable. The predicted scour hole is of similar magnitude to the observed scour hole. However it is located closer to the outside bank and its shape is elongated. Furthermore, it is noticed that the predicted point bar was of slightly lower magnitude than the observed value. It is possible that these discrepancies are due to an underestimation of the transverse bed load.

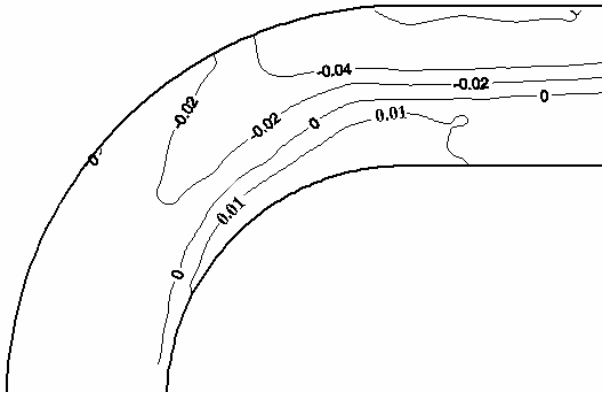

Figure 1. Predicted bed elevation contours (in meters) for 90^o channel bend without barbs

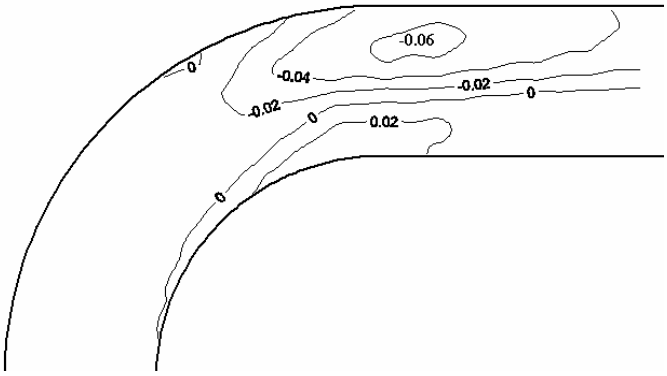

Figure 2. Measured bed elevation contours (in meters) for 90^o channel bend without barbs

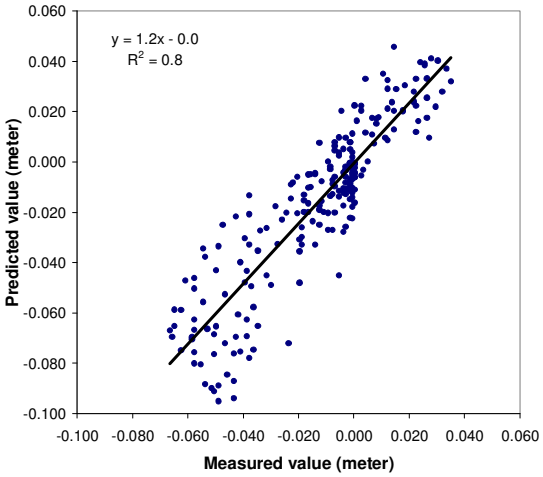

Figure 3. Predicted versus measured bed elevation for 90° channel without barbs (in meters)

A statistical comparison of the measured and predicted bed elevations for the 90° channel bend is presented in Figure 3 gives a regression coefficient of determination (r^2) of 0.8. The mean absolute deviation (M.A.D) of predicted from measured bed elevations is 0.011 meters, with a standard deviation of absolute deviation (S.D.A.D.) of 0.01 meters.

As a result of the laboratory experiments the optimum barb arrangement for the 90° and 135° channel bends was found to be Group B with a barb alignment angle of 30°. For the 90° channel this arrangement consisted of three barbs, with the first barb located 1.41 meters from the bend entrance. The three-dimensional model was used to simulate the 90° channel containing this arrangement of barbs. All parameters remained the same as the initial calibration simulation of the channel without barbs, except the simulation time was reduced to 5 hours to correspond to the time frame used during laboratory tests. Using the procedure described in [13] cells were blocked out where the barbs were located. The height, length, and slope of the barbs remained consistent with the structures used in the laboratory experiments (i.e. a height of one-half the flow depth, a length of 0.196 meters, and a 10° downward slope). However, due to limitations of the grid the width of the barbs was wider than those used in the laboratory experiments. The bed elevations, in meters, measured in the laboratory are presented in Figure 4. In comparison to Figure 1, it can be observed that the location of the thalweg has shifted away from the outer bank and the location of the deepest scour hole is located off the tip of the third barb. The bed elevations computed by the numerical model are shown in Figure 5. This figure shows similar results. In comparison to Figure 2, it can be observed that the location of the thalweg has shifted away from the outer bank and, comparable to Figure 4, the location of the deepest scour hole is located off the tip of the third barb. A statistical comparison of the measured and predicted bed elevations for the 90° channel bend containing Group B with a 30° barb alignment angle is presented in Figure 5. Figure 6 shows a regression coefficient of determination (r^2) of predicted from measured bed elevations of 0.8. The mean absolute deviation (M.A.D) of predicted from measured bed elevations is 0.008 meters, with a standard deviation of absolute deviation (S.D.A.D.) of 0.007 meters.

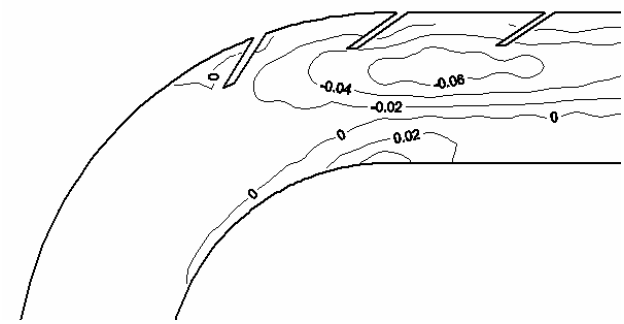

Figure 4. Measured bed elevation contours (in meters) for 90° channel bend with barbs

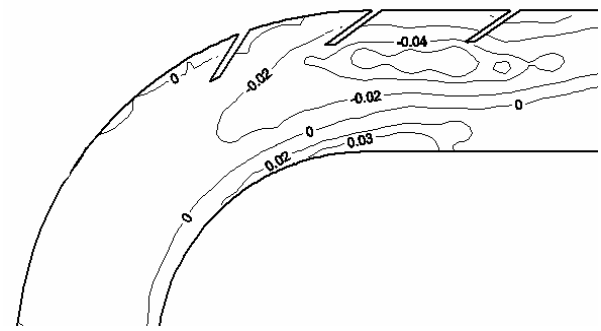

Figure 5. Predicted bed elevation contours (in meters) for 90° channel bend with barbs

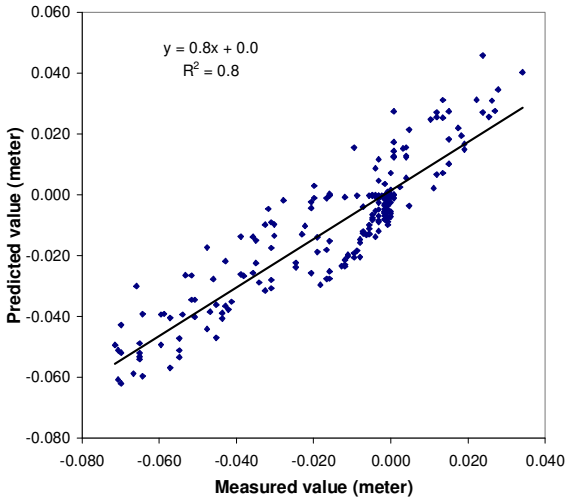

Figure 6. Predicted versus measured bed elevation for 90° channel with barbs (in meters)

Detailed measurements of the velocity field were not taken during the laboratory experiments. However, the computed velocity field for the 90° channel containing barbs was analyzed and compared to the computed velocity field for the 90° channel without barbs to observe trends in the data.

A contour map of the depth-averaged horizontal velocities, in meters per second, for the 90° channel without barbs is presented in Figure 7. It can be seen from this figure that as the flow enters the bend the location of the maximum velocity is near the center of the channel. As the flow continues through the bend, the location of the maximum velocity shifts towards the outside bank and the magnitude of velocity along the inner bank is much lower.

Figure 8 shows the depth-averaged horizontal velocity distribution for the 90° channel containing the Group B arrangement of barbs with a barb alignment angle of 30°. The location of the maximum velocity is located off the tips of the barbs, closer to the center of the channel. Therefore, with the addition of the barb arrangement to the channel, the maximum velocity does not connect with the outer bank of the channel bend. It is noted that experimental data were not available to compare to the values presented. Therefore, Figure 7 and Figure 8 are presented to suggest possible trends that relate the flow field to associated scour and deposition in a complex fluvial environment.

135° Channel

A similar procedure was used for the 135° channel bend. As a first step, the three-dimensional model was used to simulate the sediment transport and flow through the 135° channel bend without barbs in place. The structured grid for this channel bend contained 164 cells in the longitudinal direction, 18 cells in the transverse direction, and 12 cells in the vertical direction. The discharge, flow depth, channel slope, and sediment grain size remained the same as for the 90° channel bend. A simulation time of 26 hours was used. And again, a Manning number of 0.0167 and a time step of 50 seconds proved to yield favorable results. The predicted and measured bed elevations are presented in meters in Figure 9 and Figure 10, respectively. Similar to the 90° channel bend, it can be observed that sediment is being deposited along the inner bank while erosion is occurring along the outer bank. Both the measured and predicted data illustrate this trend. It can be observed that the predicted scour hole along the outer bank of the bend is smaller, and located further downstream, than the location of the measured scour hole.

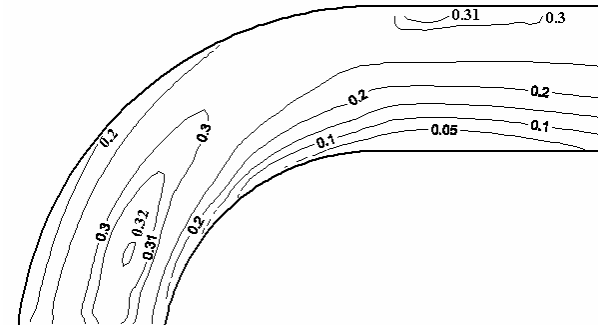

Figure 7. Depth-averaged horizontal velocity contours (in meters per second) for 90° channel bend without barbs

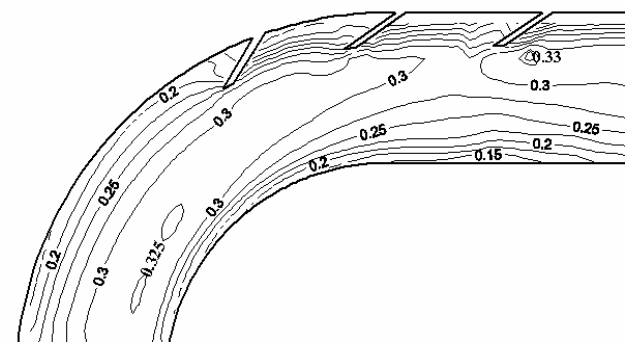

Figure 8. Depth-averaged horizontal velocity contours (in meters per second) for 90° channel bend with barbs

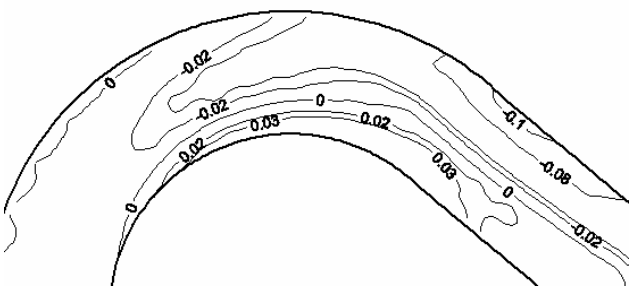

Figure 9. Predicted bed elevation contours (in meters) for 135° channel bend without barbs

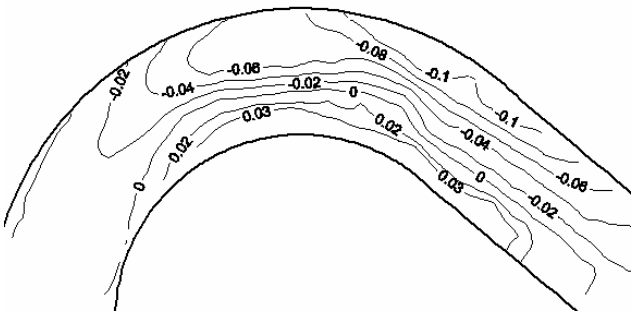

Figure 10. Measured bed elevation contours (in meters) for 135° channel bend without barbs

A statistical analysis, Figure 11, of the predicted and measured data gives a regression coefficient of determination (r^2) of predicted from measured bed elevations of 0.8, a mean absolute deviation (M.A.D) of predicted from measured bed elevations of 0.01 meters, and a standard deviation of absolute deviation (S.D.A.D.) of 0.01 meters.

The Group B arrangement of barbs with a 30° barb alignment angle consisted of 5 barbs. The first barb was located 1.41 meters from the bend entrance. The three-dimensional model was used to simulate the 135° channel containing this arrangement of barbs. All parameters remained the same as the initial calibration simulation of the channel without barbs, except the simulation time was reduced to 5 hours to correspond to the time frame used during laboratory tests.

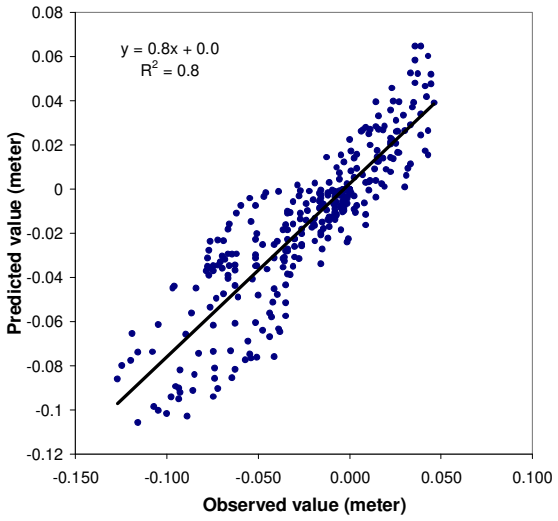

Figure 11. Predicted versus measured bed elevation for 135° channel without barbs (in meters)

The height and length of the barbs remained consistent with the structures used in the laboratory experiments (i.e. a height of one-half the flow depth, and a length of 0.196 meters). However, due to limitations of the grid the width of the barbs was wider than those used in the laboratory experiments. Furthermore, with five barbs in the channel it was not possible to replicate the slope of the barbs with the numerical model.

The measured bed elevations, in meters, are presented in Figure 12. Once again, we can see that the addition of barbs to the channel causes the thalweg to shift away from the outer bank. The location of the deepest scour hole is observed to be off the tip of the second and third barb in the grouping. The simulated bed elevations are shown in Figure 13. Similar trends can be observed in this figure. It can be seen that the thalweg has shifted towards the center of the channel. The deepest scour hole in this figure is located off the tip of the fourth barb in the grouping. The downward slope of the barbs is an important feature for their functionality. The lack of this feature for the numerical simulation could be the reason for discrepancies between the measured and predicted data. From Figure 14, the regression coefficient of determination (r^2) of predicted from measured bed elevations is 0.7. The mean absolute deviation (M.A.D) of predicted from measured bed elevations is 0.01 meters, with a standard deviation of absolute deviation (S.D.A.D.) of 0.01 meters.

A contour map of the depth-averaged horizontal velocities, in meters per second, for the 135° channel without barbs is presented in Figure 15. The depth-averaged horizontal velocities for the 135° channel with the Group B arrangement of barbs with a 30° barb alignment angle are shown in Figure 16. As with the 90° channel it can be observed that by adding the barb arrangement to the channel the location of the maximum horizontal velocity shifts away from the outer bank and towards the center of the channel. Once again it is noted

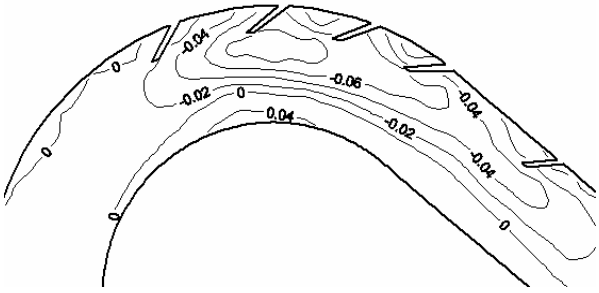

Figure 12. Measured bed elevation contours (in meters) for 135° channel bend with barbs

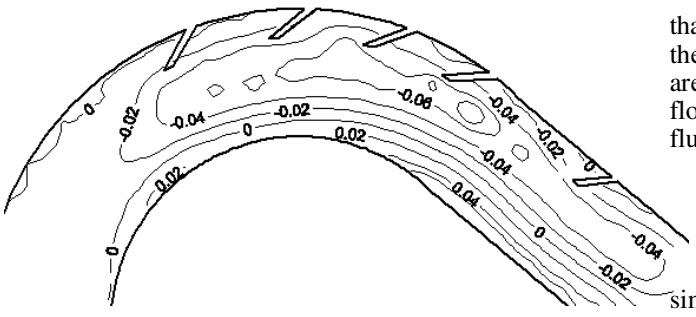

Figure 13. Predicted bed elevation contours (in meters) for 135° channel bend with barbs

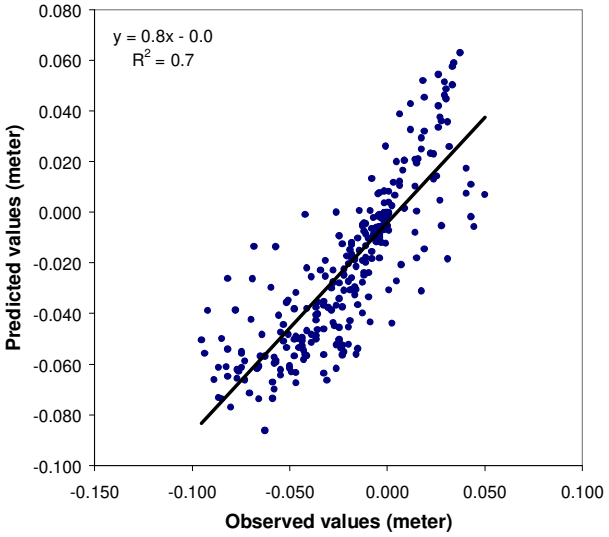

Figure 14. Predicted versus measured bed elevation for 135° channel with barbs (in meters)

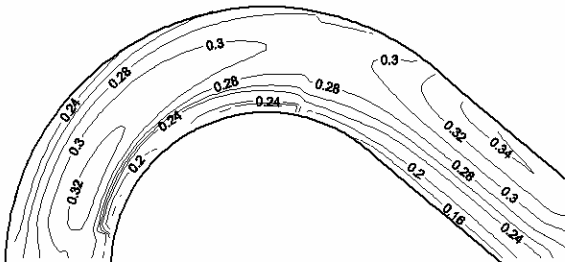

Figure 15. Depth-averaged horizontal velocity contours (in meters per second) for 135° channel bend without barbs

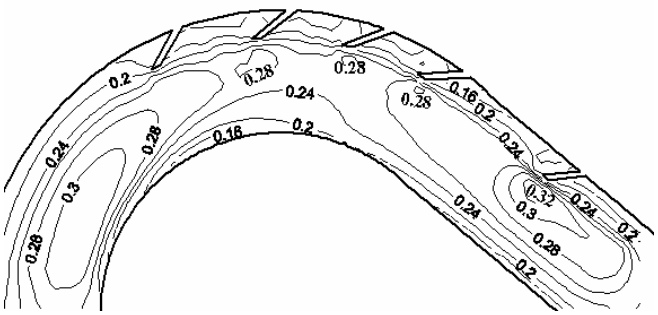

Figure 16. Depth-averaged horizontal velocity contours (in meters per second) for 135° channel bend with barbs

that experimental data were not available to compare to the predicted values. Therefore, Figure 15 and Figure 16 are presented to suggest possible trends that relate the flow field to associated scour and deposition in a complex fluvial environment.

CONCLUSIONS

A three-dimensional numerical model was used to simulate the turbulent flow field and associated scour and deposition of the bed sediments due to a series of barbs in both a 90° channel bend and a 135°channel bend. It was

observed that the results simulated by the numerical results showed good agreement with the measured data. Statistical analysis of the sediment transport results for the 90^o channel bend found a regression coefficient of determination (r^2) of predicted from measured bed elevations of 0.8 for both the channel containing the barbs and the channel without barbs. A regression coefficient of determination (r^2) of predicted from measured bed elevations of 0.7 was found for the 135^o channel containing barbs and 0.8 without barbs. The numerical model adequately simulated the important features of sediment transport through both the 90^o and 135^o channel bends (without barbs). The location and magnitude of the measured and predicted point bars and scour holes were observed to be comparable. In addition, the numerical model was able to reasonably simulate the effects of different arrangements of barb groups in the bend section. Similar to the measured results, it was observed that the location of the thalweg shifts away from the outer bank with the addition of barbs to the channel bend section. The simulated flow field data showed that the location of the maximum depth-averaged horizontal velocity moves away from the outside bank with the addition of barbs to the channel. It was observed that the maximum scour depth and horizontal velocity were located off the tips of the barbs.

There are several possible explanations for the discrepancies between the measured and predicted data. The model performed reasonably well at simulating the flow field and sediment transport through the 90^o and 135^o channel bends. However, these are complex flow fields and the three-dimensional Reynolds-averaged Navier-Stokes equations can not fully replicate secondary currents, particularly in narrow channels, due to turbulence closure. Furthermore, it was necessary to use a rigid-lid for stability of the model. Thus, it was not possible to simulate the super-elevation of the fluid along the outer bank of the channel bend. This would also reduce replication of the secondary currents due to channel curvature and pressure imbalances from the super-elevation of the fluid. As a result, it is possible that the numerical model was underestimating the transverse sediment transport.

The geometry (i.e. height, length, width, and slope) of the barbs contributes directly to its performance. It was not possible to replicate the width precisely in the model and the slope of the barbs was not included in the 135^o channel bend section. These inconsistencies in barb geometry would have contributed to discrepancies between the measured and predicted data.

REFERENCES

[1] USDA. Technical Note 23: Design of Stream Barbs. U.S. Department of Agriculture, Natural Resources Conservation Service, Portland, Oregon, April 2005.

[2] F. D. Shields, S. S. Knight, and C. M. Cooper, "Addition of spurs to stone toe protection for warmwater fish habitat rehabilitation," *J. American Water Res. Ass.*, vol. 34, pp. 1427-1436, December 1998.

[3] N. Rajaratnam and B. A. Nwachukwu, "Flow near groin-like structure," *J. Hydraulic Eng.*, vol. 109, pp. 463-480, 1983.

[4] T. Tingsanchali and S. Maherswaran, "2-D depth averaged flow computation near groyne," *J. Hydraulic Eng.*, vol. 116, pp. 71-86, January 1990.

[5] A. Molinas and Y. I. Hafez, "Finite element surface model for flow around vertical wall abutments," *J. Fluids Structures*, vol. 14, pp. 711-733, 2000.

[6] S. Ouillon and D. Dartus, "Three-dimensional computation of flow around groyne," *J. Hydraulic Eng.*, vol. 123, pp. 962-970, November 1997.

[7] W. S. J. Uijttewaal, D. Lehmann, and A. van Mazijk, "Exchange processes between a river and its groyne fields: model experiments," *J. Hydraulic Eng.*, vol. 127, pp. 928-936, November 2001.

[8] A. Sukhodolov, W. S. J. Uijttewaal, and C. Engelhardt, "On the correspondence between morphological and hydrodynamical patterns of groyne fields," *Earth Surf. Process. Landforms*, vol. 27, pp. 289-305, March, 2002.

[9] R. A. Kuhnle, C. V. Alonso, and F. D. Shields Jr, "Geometry of scour holes associated with 90º spur dikes," *J. Hydraulic Eng.*, vol. 125, pp. 972-978, September 1999.

[10] R. A. Kuhnle, C. V. Alonso, and F. D. Shields Jr., "Local scour associated with angled spur dikes," *J. Hydraulic Eng.*, vol. 128, pp. 1087-1093, December 2002.

[11] Y. Jia, S. Scott, Y. Xu, S. Huang, and S. S. Y. Wang, "Three-dimensional numerical simulation and analysis of flows around a submerged weir in a channel bendway," *J. Hydraulic Eng.*, vol. 131, pp. 682-693, August 2005.

[12] T. Matsuura, and R. Townsend, "Stream-barb installations for narrow channel bends-a laboratory study," *Can. J. Civ. Eng.*, vol. 31, pp. 478-486, June 2004.

[13] [N. R. B. Olsen, *A Three-Dimensional Numerical Model for Simulation of Sediment Movements in Water Intakes with Multiblock Option: User's Manual.* Department of Hydraulic and Environmental Engineering, Norwegian University of Science and Technology, Trondheim, Norway, 2004.

[14] S. V. Patankar, *Numerical Heat Transfer and Fluid Flow*. Hemisphere Publishing Company, Washington, USA, 1980.

[15] L. C. van Rijn, "Sediment transport. Part I: Bed load transport," *J. Hydraulic Eng.*, vol. 110, pp. 1431-1456, 1984.

[16] [USDA. Technical Note 23: Design of Stream Barbs. U.S. Department of Agriculture, Natural Resources Conservation Service, Portland, Oregon, 1999.

[17] [T. Matsuura, *Stream-Bank Protection in Narrow Channel Bends Using 'Barbs': A Laboratory Study*. M. A. Sc. Thesis, Department of Civil Engineering, University of Ottawa, Ottawa, Canada, 2004..